Predicting Long-Term Biological Dynamics from Early-Time State-Space Geometry

Arturo Tozzi *

Posted Date: 14 April 2026

doi: 10.20944/preprints202604.0982.v1

Keywords: resilience; entropy; overlap; attractor; dynamics

 doi:10.20944/preprints202604.0982.v1

Article

Predicting Long-Term Biological Dynamics from Early-Time State-Space Geometry

Arturo Tozzi

ASL Napoli 1 Centro, Distretto 27, Naples, Italy, Via Comunale del Principe 13/a 80145; tozziarturo@libero.it

Abstract

The trajectories of complex biological systems are commonly inferred from long-term observations of recovery or deviation after perturbation. We suggest that early-time state-space geometry could contain information enough to anticipate system trajectories before recovery. This hypothesis is informed by extensions of the quantum adiabatic theorem suggesting that under fast, nonadiabatic perturbations, a system prepared in its ground state within the same phase retains the largest overlap with the post-perturbation ground state. Translating to biological systems, we consider cellular functional identity as a stable attractor in a high-dimensional state space where abrupt perturbations like brief inflammatory pulses do not induce regime transitions. Our simulations suggest that post-perturbation states distribution is biased toward the original attractor, reflecting persistence of structural alignment rather than uniform exploration of accessible configurations. Early-time overlap with the baseline attractor, attractor dominance and state-space entropy could stand for operational metrics for inferring system fate. Higher initial overlap should correspond to increased return probability and reduced dispersion, whereas reduced overlap may indicate proximity to regime boundaries. We predict that system fate can be inferred from initial post-perturbation configurations without requiring long-term observation. Potential applications of our framework include fast assessment of cellular resilience, early identification of instability preceding disease transitions and optimization of intervention strategies based on early system responses.

Keywords: resilience; entropy; overlap; attractor; dynamics

Introduction

Prediction of biological systems' trajectories after perturbation is commonly addressed through longitudinal observation of recovery trajectories, with emphasis on endpoint states or steady configurations inferred from transcriptomic, proteomic or physiological data (Lüders et al. 2009; Abdulwahab et al. 2021; Kanduc 2021; Dayon et al. 2022; Werner et al. 2023). To characterize system stability and transitions, current approaches rely on dynamical systems theory, attractor reconstruction, statistical descriptors of variability, Markov blanket formulations capturing conditional dependencies among system components and temporal autocorrelation analyses to quantify memory and persistence in time series (Li et al. 2016; Parr et al. 2021; Liu et al. 2022; Li et al. 2023; Wiranata et al. 2023; Lewińska et al. 2023; Kuczynski et al. 2023). Methods like pseudotime ordering, trajectory inference and entropy-based measures have improved the description of temporal progression, yet they largely depend on post hoc reconstruction and require extended observation windows (Liu et al. 2017; Ferrario and König 2018; Miragaia et al. 2019; Setty et al. 2019; Meistermann et al. 2021; Wu et al. 2024; Senet et al. 2026). Theoretical frameworks have highlighted the role of attractor structure and basin geometry in constraining system dynamics, but operational metrics linking early perturbation responses to long-term outcomes remain limited. In physics, recent work extending the quantum adiabatic theorem has shown that even under fast, nonadiabatic perturbations, systems prepared in a ground state retain maximal overlap with the post-perturbation ground state when the phase is preserved (Damerow and Kehrein 2026). Although arising in a different domain, this result indicates that structural constraints can persist even under rapid

 doi:10.20944/preprints202604.0982.v1

perturbations. Biological research has yet to systematically translate this principle into measurable early-time indicators. It also remains unclear to what extent transient responses encode information about subsequent biological trajectories.

We suggest using early-time state-space geometry to infer system fate without relying on long-term observation. For implementation, we model cellular functional identity as a stable attractor embedded in a high-dimensional space reconstructed from gene expression profiles. Perturbations are represented as transient inputs not inducing regime transitions. We simulate a population of immune-like cells exposed to a brief inflammatory pulse, modeled as a transient increase in tumor necrosis factor. We track the coupled dynamics of gene modules associated with cellular identity and inflammatory response. We measure how closely perturbed states remain aligned with the baseline attractor using an overlap metric based on their joint distribution. We also compute complementary measures to capture attractor dominance and the spread of state distributions. Including stochastic dynamics that combine relaxation toward the baseline state with perturbation-driven deviations and noise, our setup allows comparison between structured responses and randomized controls. We expect that, shortly after perturbation, state distributions remain biased toward the original attractor, leading to higher overlap and lower dispersion than in null models without structural constraints. By varying perturbation strength, we aim to test whether this alignment changes in a graded manner and whether early-time geometry predicts return probability and reductions in state-space entropy.

We will proceed as follows. First, we define the dynamical framework and metrics to quantify overlap and distributional structure. Then, we describe the simulation protocol and parameter choices. Finally, we present the resulting trajectories and statistical analyses linking early-time geometry to system evolution.

Methods

We studied the dynamical response of a population of immune-like cells subjected to a brief inflammatory perturbation that does not induce a regime transition. Focusing on the evolution of gene expression states in a reduced space defined by identity-associated and inflammation-responsive modules, we employed stochastic differential equations to model the coupled dynamics of these modules, embedding the system in a continuous state space and incorporating both deterministic relaxation and noise. We aimed to identify an experimentally discriminable signature based on early-time geometric properties, specifically the alignment between perturbed states and the baseline attractor, quantified through overlap, return probability and entropy.

Model definition. We described each cell by a state vector $x(t) = (I(t), A(t))$, where $I(t)$ denotes the mean expression of identity-associated genes and $A(t)$ denotes the mean expression of inflammation-responsive genes, both expressed in units of $\log_2(\mathrm{CPM} + 1)$. The baseline attractor was defined as $x_0 = (I_0, A_0)$, with $I_0 = 8.0$ and $A_0 = 1.2$. The temporal evolution of each cell was modeled by a stochastic differential equation of Langevin type:

$$\frac{dx}{dt} = f(x, u(t)) + \eta(t),$$

where $f(x, u(t))$ represents deterministic dynamics under external input $u(t)$ and $\eta(t)$ is a Gaussian noise term with zero mean and covariance matrix Σ. The perturbation corresponded to a transient inflammatory pulse of finite duration $\tau_p = 1$ hand amplitude c measured in ng/mL. The system was initialized at $x(0) = x_0 + \epsilon$, where $\epsilon \sim \mathcal{N}(0, \sigma_0^2 I)$ with $\sigma_0 = 0.03$.

Deterministic dynamics. The deterministic component $f(x, u)$was defined as:

$$\frac{dI}{dt} = k_I\,(I_0 - I) \;-\; \beta \max\,[(A - A_0, 0) \;-\; \gamma\,(I - I_0)^3,$$

$$\frac{dA}{dt} = k_A\,(A_0 - A) \;+\; \alpha\,u(t) \;-\; \delta\,u(t) \max\,[(A - A_0, 0).$$

The parameters k_I and k_A define the relaxation rates toward baseline values I_0 and A_0, respectively. The coefficient α modulates the response to the external input $u(t)$, while β and δ regulate the coupling between the inflammatory and identity components. The cubic term $-\gamma\,(I -$

 doi:10.20944/preprints202604.0982.v1

$I_0)^3$ ensures local stability of the identity module by introducing a restoring nonlinearity. The rectified interaction terms based on the max operator introduce asymmetric coupling between modules, allowing the inflammatory component to influence the identity component only when exceeding its baseline level. The input function was defined as:

$$u(t) = c \cdot \mathbf{1}_{[0,\tau_p]}(t),$$

with the indicator function restricting the perturbation to the pulse interval. This formulation ensured that perturbations remained subcritical within the simulated parameter range.

Stochastic integration. The stochastic term $\eta(t)$ was modeled as:

$$\eta(t) = \begin{pmatrix} \sigma_I \xi_I(t) \\ \sigma_A \xi_A(t) \end{pmatrix},$$

where $\xi_I(t), \xi_A(t) \sim \mathcal{N}(0,1)$ are independent white noise processes and $\sigma_I = 0.05$, $\sigma_A = 0.08$. Numerical integration was performed using the Euler–Maruyama scheme:

$$x_{t+\Delta t} = x_t + f(x_t, u_t)\Delta t + \Sigma^{1/2}\sqrt{\Delta t} \cdot \zeta_t,$$

with $\zeta_t \sim \mathcal{N}(0, I)$. Time discretization was set to $\Delta t = 0.05$ h and simulations were run over $T = 48$ h. For each condition, $N = 120$ independent trajectories were generated. Reflective boundary conditions were imposed at $I = 4.5$ and $A = 0$ to maintain biologically plausible ranges.

Overlap measure. Alignment with the baseline attractor was quantified using a Gaussian overlap function:

$$O(x) = \exp\left(-\frac{1}{2}\left[\left(\frac{I - I_0}{\sigma_I'}\right)^2 + \left(\frac{A - A_0}{\sigma_A'}\right)^2\right]\right),$$

where $\sigma_I' = 0.45$, $\sigma_A' = 0.55$. The population-level overlap at time t was computed as:

$$\langle O(t) \rangle = \frac{1}{N}\sum_{i=1}^{N} O(x_i(t)).$$

This measure depends on bandwidth selection, which was fixed across all conditions to enable relative comparisons.

Return probability. Return probability was defined as the fraction of cells located within a ball of radius $r = 0.9$ centered at x_0:

$$R(t) = \frac{1}{N}\sum_{i=1}^{N} \mathbf{1}\left(\| x_i(t) - x_0 \| \leq r\right),$$

with Euclidean distance:

$$\| x - x_0 \| = \sqrt{(I - I_0)^2 + (A - A_0)^2}.$$

Entropy estimation. State-space entropy was estimated from the empirical distribution of cells over a discretized grid. Let $p_{ij}(t)$ denote the probability of finding a cell in bin (i, j) at time t. Then:

$$H(t) = -\sum_{i,j} p_{ij}(t) \log_2 p_{ij}(t).$$

Bins were defined over the intervals $I \in [4.5, 9.5]$ and $A \in [0, 6.5]$ with 24 divisions per axis. Only nonzero probabilities were included in the summation.

Null model definition. To assess whether observed alignment arises from structured dynamics rather than marginal distributions alone, a null model was built by randomizing the joint structure of the system while preserving marginal properties. At each time point t, the values of I and A were independently permuted across cells, generating surrogate datasets $\tilde{I}(t)$, $\tilde{A}(t)$ such that:

$$\tilde{I}_i(t) = I_{\pi_1(i)}(t), \tilde{A}_i(t) = A_{\pi_2(i)}(t),$$

where π_1 and π_2 are independent random permutations. This procedure preserves the marginal distributions $P(I, t)$ and $P(A, t)$ while removing correlations between variables and across trajectories. As a consequence, any residual concentration around the baseline attractor in the null model arises from marginal constraints alone rather than coordinated dynamics. Overlap, return probability and entropy were recomputed on these surrogate datasets, allowing direct comparison between structured and randomized configurations. This null model does not preserve temporal

 doi:10.20944/preprints202604.0982.v1

correlations or dynamical continuity, therefore representing a conservative baseline against which deviations due to structured dynamics can be assessed.

Simulation protocol. Simulations were conducted for pulse amplitudes $c \in \{0,2.5,5,10,14\}$ ng/mL. For each value of c, trajectories were initialized independently and evolved under identical parameters. At each time point, overlap, return probability and entropy were computed for both original and null datasets. All simulations were implemented in Python using NumPy for numerical computation and Matplotlib for visualization. Random number generation was controlled using a fixed seed to ensure reproducibility.

Results

We report the dynamical behavior of simulated cellular populations following transient inflammatory perturbations, focusing on early-time geometric properties, their evolution over time and their relationship to recovery trajectories and distributional structure, including comparison with the null model.

Early alignment. Immediately after the onset of the perturbation, trajectories diverged from the baseline attractor in a dose-dependent manner, with larger displacements observed at higher TNF concentrations, while remaining confined within a restricted region of state space (Figure 1). Quantification of alignment through the overlap measure showed a rapid decrease during the pulse phase, followed by a monotonic recovery toward baseline values across all subcritical perturbations (Figure 2). At early time points, overlap values remained consistently above zero for all tested conditions, including the highest dose, indicating persistent alignment with the baseline attractor. In contrast, the null model exhibited a broader distribution with reduced density near the attractor and lower overlap values at corresponding time points. This difference was most evident immediately after the perturbation, where structured simulations retained a concentrated distribution, whereas null configurations displayed increased dispersion due to the removal of correlations. The magnitude of overlap reduction scaled with perturbation strength in both cases, but the structured system systematically maintained higher overlap than the null model across all time points. These results indicate that early-time dynamics preserve coordinated structure that is not captured by marginal distributions alone, establishing a measurable separation between structured and randomized responses.

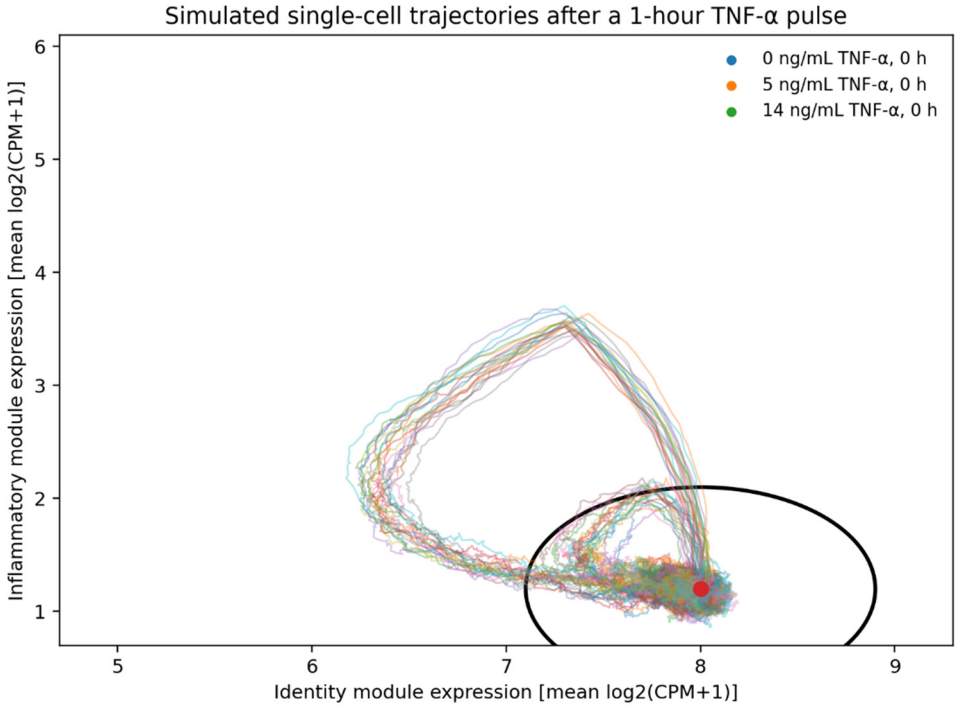

 doi:10.20944/preprints202604.0982.v1

Figure 1. Simulated single-cell trajectories after a 1-hour TNF-α pulse at 0, 5 or 14 ng/mL. The circle marks the baseline attractor basin centered on the pre-perturbation state. Mild and intermediate pulses displace cells toward inflammatory activation with partial preservation of identity, whereas higher doses produce larger transient excursions away from the baseline basin before recovery.

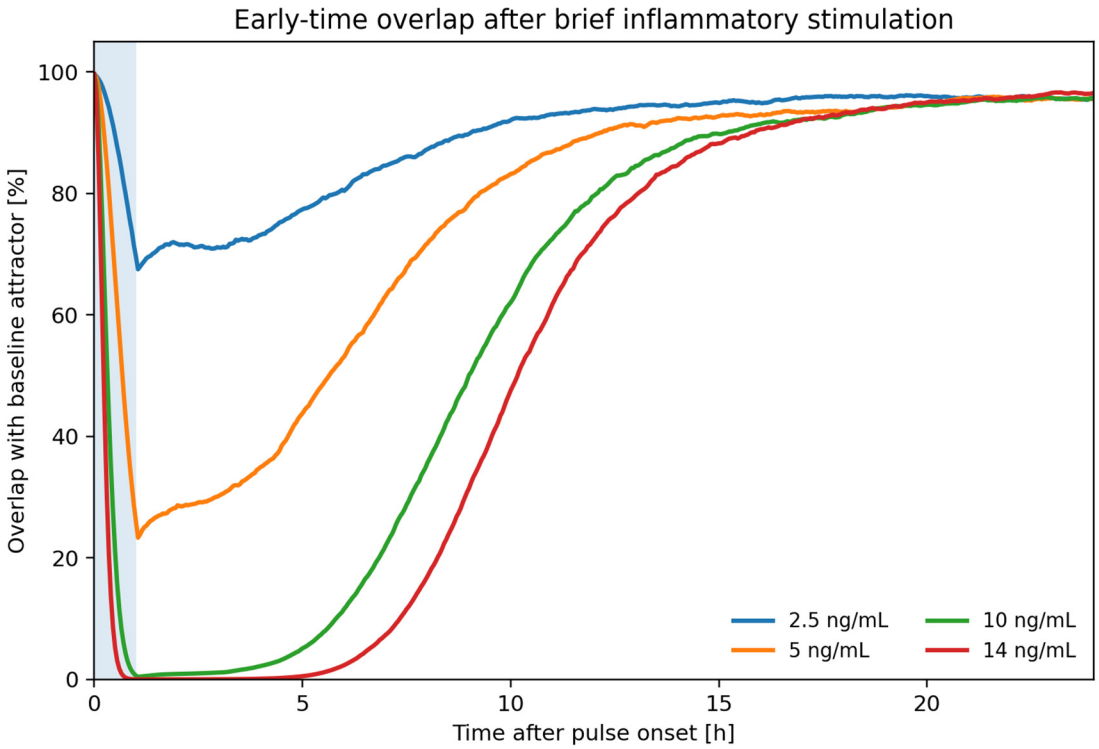

Figure 2. Mean overlap with the baseline attractor plotted over 24 hours after 1-hour TNF-α pulses of 2.5, 5, 10 and 14 ng/mL. Overlap is expressed as percent similarity to the baseline attractor computed from the joint distribution of identity and inflammatory module expression. All conditions show an early drop followed by recovery, but stronger pulses produce lower initial overlap and slower return, indicating greater transient deviation despite preservation of the same dynamical regime.

Recovery structure. The fraction of cells located within the baseline attractor basin decreased during the perturbation phase and subsequently increased during recovery, with distinct temporal profiles across concentrations (Figure 3). Lower concentrations maintained higher basin occupancy throughout the trajectory, whereas higher concentrations exhibited delayed re-entry and reduced occupancy at intermediate times. At 24 hours, return probability decreased progressively with increasing perturbation amplitude, while remaining above zero for all conditions. In the null model, basin occupancy remained consistently lower and showed weaker recovery, reflecting the absence of coordinated trajectories. State-space entropy increased with perturbation strength in both structured and null systems; however, entropy values were systematically higher in the null model, indicating broader dispersion when correlations were removed. The inverse relationship between return probability and entropy was preserved across conditions, but the structured system maintained lower entropy and higher basin occupancy at matched doses. Trajectories exhibiting higher early-time overlap corresponded to higher basin occupancy and lower entropy at later time points, whereas trajectories with reduced early overlap showed increased dispersion and slower convergence. These observations show that early geometric alignment is quantitatively associated with subsequent distributional evolution and that this association depends on coordinated dynamics beyond marginal constraints.

 doi:10.20944/preprints202604.0982.v1

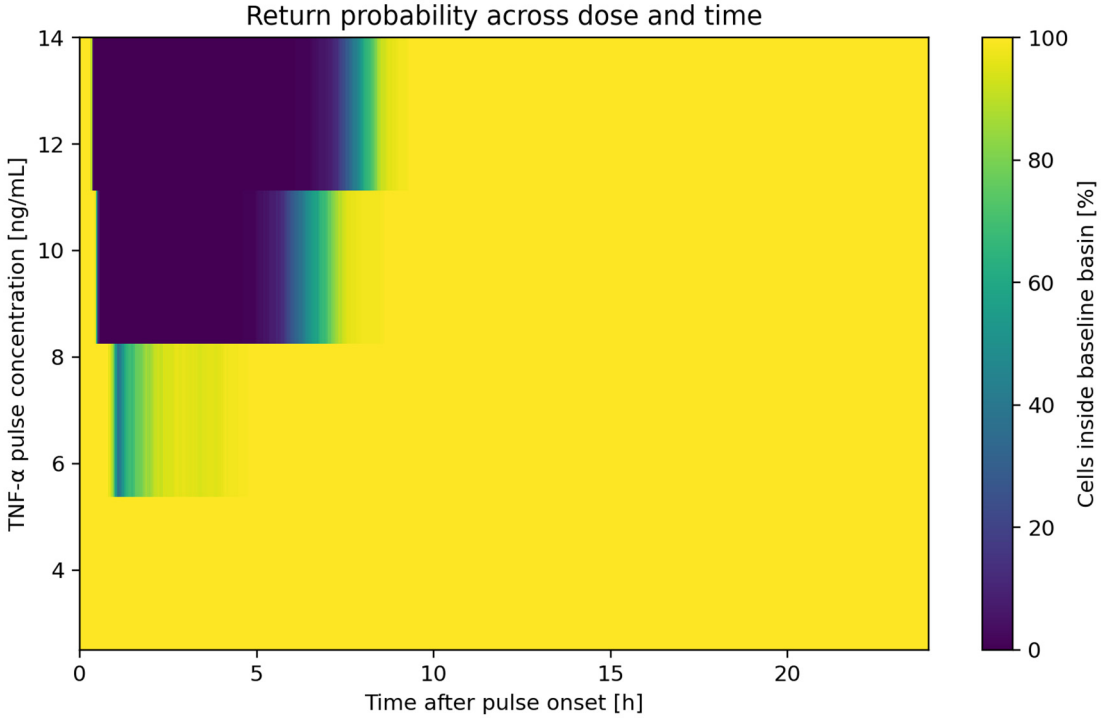

Figure 3. Heat mapping showing the percentage of cells located inside the baseline attractor basin as a function of time after pulse onset and TNF-α concentration. Lower concentrations maintain higher basin occupancy throughout recovery, whereas higher concentrations induce broader early displacement and delayed re-entry. This pattern identifies a graded loss of early attractor dominance without a complete regime transition across the simulated dose range.

Overall, we show that transient perturbations induce deviations biased toward the baseline attractor and that early-time geometric alignment is systematically related to later recovery dynamics. The observed relationships between overlap, return probability and entropy shows that initial state-space configuration encodes information about system evolution within preserved regimes.

Conclusions

We asked whether the outcomes of a biological system subjected to transient perturbation can be inferred from its early-time state-space configuration rather than from long-term observation. Our simulations compared populations of cells exposed to brief inflammatory pulses of varying amplitude, tracking their trajectories in a reduced gene-expression space and quantifying alignment with a baseline attractor through overlap, return probability and entropy. We found that, immediately after perturbation, state distributions remain non-uniform and preferentially aligned with the baseline configuration, with the degree of early alignment systematically related to subsequent recovery dynamics. Stronger perturbations produced larger deviations and broader distributions, yet within the same regime the system retained a structured bias toward the original attractor. These results are consistent with an interpretation in which early-time geometry is associated with latent constraints that shape later evolution, indicating that the initial post-perturbation configuration is not arbitrary but retains information about system stability. This association was not reproduced by the null model, suggesting that it depends on coordinated structure beyond marginal distributions. Therefore, system fate could be approached as a problem of geometric alignment at early times, rather than an outcome observable after extended evolution.

Compared with existing approaches relying on trajectory reconstruction or endpoint classification, we introduce a directly computable quantity based on early-time configurations, namely the overlap with a reference attractor and its associated distributional measures. This

 doi:10.20944/preprints202604.0982.v1

provides a means to evaluate system behavior without requiring full temporal trajectories or steady-state convergence. Our approach differs from standard dynamical analyses by focusing on the geometry of distributions rather than on inferred pathways. Yielding measurable quantities that can be derived from single time points or short temporal windows, it extends current capabilities in dynamical modeling.

Our study has several limitations. It should be interpreted within the limits of a model with non-calibrated parameters and kernel-dependent measures, representing a class of constrained stochastic dynamics rather than as a validated predictive description of specific biological systems. No explicit potential or Lyapunov function is specified, so stability properties are assumed rather than formally demonstrated. Nonlinear terms, including cubic stabilization and rectified interactions, are not calibrated against experimental measurements. Parameter choices like inflammatory input scaling and noise amplitudes are not empirically grounded. The overlap metric relies on a Gaussian kernel with fixed bandwidths that directly influence results, while entropy estimates depend on discretization choices that introduce bias. The analogy with the quantum adiabatic theorem is just conceptual and not supported by a formal mapping.

Testable hypotheses follow from our framework. First, early-time alignment predicts recovery: for a fixed perturbation duration, the mean overlap at $t = 2\,\mathrm{h}$, $\langle O(2\,\mathrm{h})\rangle$, should positively correlate with return probability at $t = 24\,\mathrm{h}$, $R(24\,\mathrm{h})$. A measurable expectation is a monotonic relation $\partial R / \partial \langle O\rangle > 0$ across doses, with a regression slope remaining positive under resampling.

Second, overlap decay scales with perturbation amplitude c (ng/mL): the minimum overlap $O_{\min}$ during the pulse should satisfy $O_{\min} \approx \exp[-kc]$ for moderate c, with k estimated from data and compared across cell types.

Third, dispersion grows with dose: state-space entropy at $t = 2\,\mathrm{h}$, $H(2\,\mathrm{h})$, should increase approximately linearly with c within the same regime, while $R(24\,\mathrm{h})$ decreases accordingly.

Fourth, a threshold-like behavior is expected: there exists c^* such that the attractor dominance ratio $D(24\,\mathrm{h})$ approaches unity as $c \to c^*$, indicating proximity to a regime boundary.

Fifth, kernel robustness can be assessed: varying bandwidths (σ_I, σ_A) should preserve rank ordering of conditions in $\langle O(2\,\mathrm{h})\rangle$ if the signal is not an artifact.

Future work should derive dynamics directly from time-resolved data using drift and diffusion estimation, replace fixed-kernel overlap with likelihood-based or transport-based distances and build rigorously defined null models preserving marginals and temporal autocorrelation. Extensions could include higher-dimensional embeddings, patient-specific parameter inference and systematic evaluation near regime transitions to test the predicted threshold behavior.

Open questions include how to derive the governing dynamics from data, how to define overlap metrics independent of kernel choices and how early-time geometry behaves near regime transitions.

Our approach enables short time-window measurements to inform decision-making in experimental and clinical settings where rapid assessment is required. By extracting quantitative descriptors from early observations, it becomes possible to stratify samples, compare interventions and rank perturbations without waiting for full temporal evolution. This allows implementation in high-throughput platforms where repeated long-term measurements are impractical, reducing experimental cost and time. In clinical contexts, early readouts from minimally invasive assays could be used to guide treatment selection or adjust dosing strategies in near real time. Our method is compatible with existing data acquisition pipelines, single-cell transcriptomics, targeted panels and computational workflows for automated analysis.

In conclusion, we examined whether short-term observations following transient perturbations may contain information about subsequent system behavior. Using stochastic simulations of coupled gene-expression modules, we quantified how early configurations relate to later outcomes through measurable descriptors. We conclude that initial post-perturbation states may retain structured information related to later dynamics, although this depends on the model assumptions. This suggests that early observations could provide partial insight into system evolution when underlying conditions are preserved.

 doi:10.20944/preprints202604.0982.v1

Authors' contributions: The Author performed: study concept and design, acquisition of data, analysis and interpretation of data, drafting of the manuscript, critical revision of the manuscript for important intellectual content, statistical analysis, obtained funding, administrative, technical and material support, study supervision.

Funding: This research did not receive any specific grant from funding agencies in the public, commercial or not-for-profit sectors.

Ethics approval and consent to participate: This research does not contain any studies with human participants or animals performed by the Author.

Consent for publication: The Author transfers all copyright ownership, in the event the work is published. The undersigned author warrants that the article is original, does not infringe on any copyright or other proprietary right of any third part, is not under consideration by another journal and has not been previously published.

Availability of data and materials: All data and materials generated or analyzed during this study are included in the manuscript. The Author had full access to all the data in the study and took responsibility for the integrity of the data and the accuracy of the data analysis.

Declaration of generative AI and AI-assisted technologies in the writing process: During the preparation of this work, the author used ChatGPT 5.3 to assist with data analysis and manuscript drafting and to improve spelling, grammar and general editing. After using this tool, the author reviewed and edited the content as needed, taking full responsibility for the content of the publication.

Acknowledgements: none.

Disclaimer. The views expressed are those of the author and do not necessarily reflect those of the affiliated institutions.

Competing interests. The Author does not have any known or potential conflict of interest including any financial, personal or other relationships with other people or organizations within three years of beginning the submitted work that could inappropriately influence or be perceived to influence their work.

References

Abdulwahab, H., M. Aljishi, A. Sultan, G. Al-Kafaji, K. Sridharan, et al. 2021. "Whole Blood Transcriptomic Analysis Reveals PLSCR4 as a Potential Marker for Vaso-Occlusive Crises in Sickle Cell Disease." *Scientific Reports* 11 (1): 22199. https://doi.org/10.1038/s41598-021-01702-8.

Damerow, S., and S. Kehrein. 2026. "Extension of the Adiabatic Theorem." *Physical Review B* 113: 165102.

Dayon, L., O. Cominetti, and M. Affolter. 2022. "Proteomics of Human Biological Fluids for Biomarker Discoveries: Technical Advances and Recent Applications." *Expert Review of Proteomics* 19 (2): 131–151. https://doi.org/10.1080/14789450.2022.2070477.

Ferrario, P. G., and I. R. König. 2018. "Transferring Entropy to the Realm of GxG Interactions." *Briefings in Bioinformatics* 19 (1): 136–147. https://doi.org/10.1093/bib/bbw086.

Kanduc, D. 2021. "The Role of Proteomics in Defining Autoimmunity." *Expert Review of Proteomics* 18 (3): 177–184. https://doi.org/10.1080/14789450.2021.1914595.

Kuczynski, L., V. J. Ontiveros, and H. Hillebrand. 2023. "Biodiversity Time Series Are Biased towards Increasing Species Richness in Changing Environments." *Nature Ecology & Evolution* 7 (7): 994–1001. https://doi.org/10.1038/s41559-023-02078-w.

Lewińska, K. E., A. R. Ives, C. J. Morrow, N. Rogova, H. Yin, et al. 2023. "Beyond 'Greening' and 'Browning': Trends in Grassland Ground Cover Fractions across Eurasia That Account for Spatial and Temporal Autocorrelation." *Global Change Biology* 29 (16): 4620–4637. https://doi.org/10.1111/gcb.16800.

Li, H., Z. Yuan, J. Ji, J. Xu, T. Zhang, et al. 2016. "A Novel Markov Blanket-Based Repeated-Fishing Strategy for Capturing Phenotype-Related Biomarkers in Big Omics Data." *BMC Genetics* 17: 51. https://doi.org/10.1186/s12863-016-0358-5.

Li, J., M. J. Hubisz, E. M. Earlie, M. A. Duran, C. Hong, et al. 2023. "Non-Cell-Autonomous Cancer Progression from Chromosomal Instability." *Nature* 620 (7976): 1080–1088. https://doi.org/10.1038/s41586-023-06464-z.

 doi:10.20944/preprints202604.0982.v1

Liu, H., R. Zhao, H. Fang, F. Cheng, Y. Fu, and Y. Y. Liu. 2017. "Entropy-Based Consensus Clustering for Patient Stratification." *Bioinformatics* 33 (17): 2691–2698. https://doi.org/10.1093/bioinformatics/btx167.

Liu, W., Y. Jiang, L. Peng, X. Sun, W. Gan, et al. 2022. "Inferring Gene Regulatory Networks Using the Improved Markov Blanket Discovery Algorithm." *Interdisciplinary Sciences* 14 (1): 168–181. https://doi.org/10.1007/s12539-021-00478-9.

Lüders, S., C. Fallet, and E. Franco-Lara. 2009. "Proteome Analysis of the Escherichia coli Heat Shock Response under Steady-State Conditions." *Proteome Science* 7: 36. https://doi.org/10.1186/1477-5956-7-36.

Meistermann, D., A. Bruneau, S. Loubersac, A. Reignier, J. Firmin, V, et al. 2021. "Integrated Pseudotime Analysis of Human Pre-Implantation Embryo Single-Cell Transcriptomes Reveals the Dynamics of Lineage Specification." *Cell Stem Cell* 28 (9): 1625–1640.e6. https://doi.org/10.1016/j.stem.2021.04.027.

Miragaia, R. J., T. Gomes, A. Chomka, L. Jardine, A. Riedel, et al. 2019. "Single-Cell Transcriptomics of Regulatory T Cells Reveals Trajectories of Tissue Adaptation." *Immunity* 50 (2): 493–504.e7. https://doi.org/10.1016/j.immuni.2019.01.001.

Parr, T., L. Da Costa, C. Heins, M. J. D. Ramstead, and K. J. Friston. 2021. "Memory and Markov Blankets." *Entropy* 23 (9): 1105. https://doi.org/10.3390/e23091105.

Senet, P., A. Guzzo, P. Delarue, C. Laforge, G. G. Maisuradze, et al. 2026. "Local Entropy in Proteins." *Chemical Science* 17 (11): 5482–5497. https://doi.org/10.1039/d5sc06411b.

Setty, M., V. Kiseliovas, J. Levine, A. Gayoso, L. Mazutis, and D. Pe'er. 2019. "Characterization of Cell Fate Probabilities in Single-Cell Data with Palantir." *Nature Biotechnology* 37 (4): 451–460. https://doi.org/10.1038/s41587-019-0068-4.

Werner, T., M. Fahrner, and O. Schilling. 2023. "Using Proteomics for Stratification and Risk Prediction in Patients with Solid Tumors." *Pathologie* 44 (Suppl 3): 176–182. https://doi.org/10.1007/s00292-023-01261-x.

Wiranata, J. A., H. Puspitaningtyas, S. H. Hutajulu, J. Fachiroh, N. Anggorowati, et al. 2023. "Temporal and Spatial Analyses of Colorectal Cancer Incidence in Yogyakarta, Indonesia: A Cross-Sectional Study." *Geospatial Health* 18 (1). https://doi.org/10.4081/gh.2023.1186.

Wu, L. P., L. Yong, X. Cheng, and Y. Zhou. 2024. "Research on Similarity Retrieval Method Based on Mass Spectral Entropy." *Journal of Bioinformatics and Computational Biology* 22 (6): 2450027. https://doi.org/10.1142/S0219720024500276.